

A Family of Virtual Element Methods for Plane Elasticity Problems Based on the Hellinger-Reissner Principle

E. Artioli*, S. de Miranda†, C. Lovadina‡, L. Patruno§

Abstract

A family of Virtual Element schemes based on the Hellinger-Reissner variational principle is presented. A convergence and stability analysis is rigorously developed. Numerical tests confirming the theoretical predictions are performed.

1 Introduction

In this paper we extend the study presented in our previous paper [4]. More precisely, we design and study higher-order Virtual Element Methods (VEM) to approximate the solution of linear elasticity problems in 2D. We take the Hellinger-Reissner variational principle (see [18] or [10], for instance) as the basis of the discretization procedure. As it is well-known, imposing both the symmetry of the stress tensor and the continuity of the tractions at the inter-element is typically a great source of troubles in the framework of classical Galerkin schemes. For example, when Finite Element Methods are employed, one is essentially led to adopt either cumbersome elements, or to relax the stress symmetry (this latter choice means that the underlying variational principle is changed). The reason for this difficulty stands in the local polynomial approximation that can not easily accomplish for both the symmetry and continuity constraints mentioned above. More details about this issue can be found in [10].

As in [4], we exploit the great flexibility of VEM to present alternative methods, which provide symmetric stresses, continuous tractions and are reasonably cheap with respect to the delivered accuracy. VEMs reach this goal by abandoning the local polynomial approximation concept, a feature originally used to design conforming Galerkin schemes on general polytopal meshes, see [8]. Recently, this property has been found useful, in certain situations, for the numerical treatment of internal or regularity constraints, such as incompressibility or inter-element regularity (see [9], [7]).

We also remark that VEM is experiencing a growing interest towards the applications to Structural Mechanics problems (see [17, 15, 2, 3, 23, 14, 1] and [5, 13], for example). Thus, this paper represents a contribution along that line.

An outline of the paper is as follows. In Section 2 we introduce the 2D elasticity problem using the mixed Hellinger-Reissner formulation. Section 3 details the discrete

*Department of Civil Engineering and Computer Science, University of Rome Tor Vergata, Via del Politecnico 1, 00133 Rome, Italy, artioli@ing.uniroma2.it

†DICAM, University of Bologna, Viale Risorgimento 2, 40136 Bologna, Italy, stefano.demiranda@unibo.it

‡Dipartimento di Matematica, Università di Milano, Via Saldini 50, 20133 Milano, and IMATI del CNR, Via Ferrata 1, 27100 Pavia, Italy, carlo.lovadina@unimi.it

§DICAM, University of Bologna, Viale Risorgimento 2, 40136 Bologna, Italy, luca.patruno@unibo.it

methods, by describing all the relevant projectors, bilinear and linear forms, together with the VEM approximation spaces. The stability and convergence analysis is developed in Section 4, while numerical experiments are provided in Section 5. Concluding considerations are given in Section 6.

Throughout the paper, given two quantities a and b , we use the notation $a \lesssim b$ to mean: there exists a constant C , independent of the mesh-size, such that $a \leq Cb$. In addition, given a set $\omega \subseteq \mathbb{R}$ (or $\omega \subseteq \mathbb{R}^2$), we denote with $\mathcal{P}_k(\omega)$ the space of polynomials up to degree k defined on ω . Moreover, we use standard notations for Sobolev spaces, norms and semi-norms (cf. [19], for example).

2 The linear 2D elasticity problem

It is well-known, see for example [10, 11], that the linear elasticity problem reads as follows.

$$\begin{cases} \text{Find } (\boldsymbol{\sigma}, \mathbf{u}) \text{ such that} \\ -\operatorname{div} \boldsymbol{\sigma} = \mathbf{f} & \text{in } \Omega \\ \boldsymbol{\sigma} = \mathbb{C}\boldsymbol{\varepsilon}(\mathbf{u}) & \text{in } \Omega \\ \mathbf{u}|_{\partial\Omega} = \mathbf{0} \end{cases} \quad (1)$$

where homogeneous Dirichlet boundary conditions are here chosen only for the sake of simplicity. However, different conditions can be treated in standard ways. Introducing the L^2 scalar product (\cdot, \cdot) , and $a(\boldsymbol{\sigma}, \boldsymbol{\tau}) := (\mathbb{D}\boldsymbol{\sigma}, \boldsymbol{\tau})$, a mixed variational formulation of the problem is:

$$\begin{cases} \text{Find } (\boldsymbol{\sigma}, \mathbf{u}) \in \Sigma \times U \text{ such that} \\ a(\boldsymbol{\sigma}, \boldsymbol{\tau}) + (\operatorname{div} \boldsymbol{\tau}, \mathbf{u}) = 0 \quad \forall \boldsymbol{\tau} \in \Sigma \\ (\operatorname{div} \boldsymbol{\sigma}, \mathbf{v}) = -(\mathbf{f}, \mathbf{v}) \quad \forall \mathbf{v} \in U. \end{cases} \quad (2)$$

In this paper we confine to consider polygonal domains $\Omega \subset \mathbb{R}^2$. Furthermore, we set $\Sigma = H(\operatorname{div}; \Omega)$, $U = L^2(\Omega)^2$, and we suppose that $\mathbf{f} \in L^2(\Omega)^2$. The elasticity fourth-order symmetric tensor $\mathbb{D} := \mathbb{C}^{-1}$ is assumed to be uniformly bounded, positive-definite and sufficiently regular. After having introduced a polygonal mesh \mathcal{T}_h of meshsize h , the bilinear form $a(\cdot, \cdot)$ in (2) can be split as

$$a(\boldsymbol{\sigma}, \boldsymbol{\tau}) = \sum_{E \in \mathcal{T}_h} a_E(\boldsymbol{\sigma}, \boldsymbol{\tau}) \quad \text{with} \quad a_E(\boldsymbol{\sigma}, \boldsymbol{\tau}) := \int_E \mathbb{D}\boldsymbol{\sigma} : \boldsymbol{\tau} \quad \forall \boldsymbol{\sigma}, \boldsymbol{\tau} \in \Sigma. \quad (3)$$

Similarly, it holds

$$(\operatorname{div} \boldsymbol{\tau}, \mathbf{v}) = \sum_{E \in \mathcal{T}_h} (\operatorname{div} \boldsymbol{\tau}, \mathbf{v})_E \quad \text{with} \quad (\operatorname{div} \boldsymbol{\tau}, \mathbf{v})_E := \int_E \operatorname{div} \boldsymbol{\tau} \cdot \mathbf{v} \quad \forall (\boldsymbol{\tau}, \mathbf{v}) \in \Sigma \times U. \quad (4)$$

The divergence-free space is defined by:

$$K = \{\boldsymbol{\tau} \in \Sigma : (\operatorname{div} \boldsymbol{\tau}, \mathbf{v}) = 0 \quad \forall \mathbf{v} \in U\}. \quad (5)$$

3 The Virtual Element Methods

In this section we define our Virtual Element discretization of Problem (2). Let $\{\mathcal{T}_h\}_h$ be a sequence of decompositions of Ω into general polygonal elements E with

$$h_E := \operatorname{diameter}(E), \quad h := \sup_{E \in \mathcal{T}_h} h_E.$$

We suppose that for all h , each element E in \mathcal{T}_h fulfils the following assumptions:

- **(A1)** E is star-shaped with respect to a ball of radius $\geq \gamma h_E$,
- **(A2)** the distance between any two vertexes of E is $\geq c h_E$,

where γ and c are positive constants. The hypotheses above, and in particular **(A2)**, may be relaxed (see [6], where a scalar elliptic model problem in primal form is considered).

3.1 The local spaces

We first fix an integer $k \geq 1$. Given a polygon $E \in \mathcal{T}_h$ with n_E edges, we introduce the space of local infinitesimal rigid body motions:

$$RM(E) = \left\{ \mathbf{r}(\mathbf{x}) = \mathbf{a} + b(\mathbf{x} - \mathbf{x}_C)^\perp \quad \mathbf{a} \in \mathbb{R}^2, \quad b \in \mathbb{R} \right\}. \quad (6)$$

Above, given $\mathbf{c} = (c_1, c_2)^T \in \mathbb{R}^2$, \mathbf{c}^\perp is the clock-wise rotated vector $\mathbf{c}^\perp = (c_2, -c_1)^T$, and \mathbf{x}_C is the centroid of E . We also introduce the space

$$RM_k^\perp(E) = \left\{ \mathbf{p}_k(\mathbf{x}) \in \mathcal{P}_k(E)^2 : \int_E \mathbf{p}_k \cdot \mathbf{r} = 0 \quad \forall \mathbf{r} \in RM(E) \right\}. \quad (7)$$

Hence, the following L^2 -orthogonal decomposition holds:

$$\mathcal{P}_k(E)^2 = RM(E) \oplus RM_k^\perp(E). \quad (8)$$

Our local approximation space for the stress field is then defined by

$$\begin{aligned} \Sigma_h(E) = \left\{ \boldsymbol{\tau}_h \in H(\mathbf{div}; E) : \exists \mathbf{w}^* \in H^1(E)^2 \text{ such that } \boldsymbol{\tau}_h = \mathbb{C}\boldsymbol{\varepsilon}(\mathbf{w}^*); \right. \\ \left. (\boldsymbol{\tau}_h \mathbf{n})|_e \in \mathcal{P}_k(e)^2 \quad \forall e \in \partial E; \quad \mathbf{div} \boldsymbol{\tau}_h \in \mathcal{P}_k(E)^2 \right\}. \end{aligned} \quad (9)$$

Remark 1. *Alternatively, the space (9) can be defined as follows.*

$$\begin{aligned} \Sigma_h(E) = \left\{ \boldsymbol{\tau}_h \in H(\mathbf{div}; E) : \boldsymbol{\tau}_h = \boldsymbol{\tau}_h^T; \quad \text{curl} \, \text{curl}(\mathbb{D}\boldsymbol{\tau}_h) = 0; \right. \\ \left. (\boldsymbol{\tau}_h \mathbf{n})|_e \in \mathcal{P}_k(e)^2 \quad \forall e \in \partial E; \quad \mathbf{div} \boldsymbol{\tau}_h \in \mathcal{P}_k(E)^2 \right\}. \end{aligned} \quad (10)$$

Here above, the equation $\text{curl} \, \text{curl}(\mathbb{D}\boldsymbol{\tau}_h) = 0$ is to be intended in the distribution sense.

We remark that, due to the decomposition (8), we may write $\mathbf{div} \boldsymbol{\tau}_h = \mathbf{r}_\boldsymbol{\tau} + \mathbf{p}_\boldsymbol{\tau}$ for a unique couple $(\mathbf{r}_\boldsymbol{\tau}, \mathbf{p}_\boldsymbol{\tau}) \in RM(E) \times RM_k^\perp(E)$.

We now notice that the $RM(E)$ -component $\mathbf{r}_\boldsymbol{\tau}$ of $\mathbf{div} \boldsymbol{\tau}_h$ is completely determined once $(\boldsymbol{\tau}_h \mathbf{n})|_e := \mathbf{p}_{k,e} \in \mathcal{P}_k(e)^2$ is given for all $e \in \partial E$. Indeed, let us denote with $\boldsymbol{\varphi} : \partial E \rightarrow \mathbb{R}^2$ the function such that $\boldsymbol{\varphi}|_e := \mathbf{p}_{k,e}$. Using the obvious compatibility condition and the orthogonal decomposition (8), we have:

$$\int_E \mathbf{r}_\boldsymbol{\tau} \cdot \mathbf{r} = \int_E \mathbf{div} \boldsymbol{\tau}_h \cdot \mathbf{r} = \int_{\partial E} \boldsymbol{\tau}_h \mathbf{n} \cdot \mathbf{r} = \int_{\partial E} \boldsymbol{\varphi} \cdot \mathbf{r} \quad \forall \mathbf{r} \in RM(E), \quad (11)$$

which allows to compute $\mathbf{r}_\boldsymbol{\tau}$ using the $\mathbf{p}_{k,e}$'s. More precisely, setting (cf (6))

$$\mathbf{r}_\boldsymbol{\tau} = \boldsymbol{\alpha}_E + \beta_E(\mathbf{x} - \mathbf{x}_C)^\perp, \quad (12)$$

from (11) we infer

$$\begin{cases} \alpha_E = \frac{1}{|E|} \int_{\partial E} \varphi = \frac{1}{|E|} \sum_{e \in \partial E} \int_e \mathbf{p}_{k,e} \\ \beta_E = \frac{1}{\int_E |\mathbf{x} - \mathbf{x}_C|^2} \int_{\partial E} \varphi \cdot (\mathbf{x} - \mathbf{x}_C)^\perp = \frac{1}{\int_E |\mathbf{x} - \mathbf{x}_C|^2} \sum_{e \in \partial E} \int_e \mathbf{p}_{k,e} \cdot (\mathbf{x} - \mathbf{x}_C)^\perp. \end{cases} \quad (13)$$

The equations above suggest to take the following functionals as degrees of freedom in $\Sigma_h(E)$.

- For each edge $e \in \partial E$, given $\boldsymbol{\tau}_h \in \Sigma_h(E)$:

$$\boldsymbol{\tau}_h \longrightarrow \int_e \boldsymbol{\tau}_h \mathbf{n} \cdot \mathbf{p}_k \quad \forall \mathbf{p}_k \in \mathcal{P}_k(e)^2. \quad (14)$$

- In the polygon E , given $\boldsymbol{\tau}_h \in \Sigma_h(E)$:

$$\boldsymbol{\tau}_h \longrightarrow \int_E \mathbf{div} \boldsymbol{\tau}_h \cdot \boldsymbol{\psi}_k \quad \forall \boldsymbol{\psi}_k \in RM_k^\perp(E). \quad (15)$$

Indeed, we have:

Lemma 3.1. *If $\boldsymbol{\tau}_h \in \Sigma_h(E)$, then*

$$\begin{cases} \int_e \boldsymbol{\tau}_h \mathbf{n} \cdot \mathbf{p}_k = 0 & \forall \mathbf{p}_k \in \mathcal{P}_k(e)^2, \quad \forall e \in \partial E; \\ \int_E \mathbf{div} \boldsymbol{\tau}_h \cdot \boldsymbol{\psi}_k = 0 & \forall \boldsymbol{\psi}_k \in RM_k^\perp(E), \end{cases} \quad (16)$$

imply $\boldsymbol{\tau}_h = \mathbf{0}$.

Proof. The first (boundary) conditions of (16) leads to infer, see (12) and (13):

$$\boldsymbol{\tau}_h \mathbf{n} = \mathbf{0} \quad \text{on } \partial E, \quad \mathbf{div} \boldsymbol{\tau}_h \in RM_k^\perp(E). \quad (17)$$

From (17) and the second set of conditions in (16), we deduce $\mathbf{div} \boldsymbol{\tau}_h = \mathbf{0}$. Therefore, $\boldsymbol{\tau}_h \in \Sigma_h(E)$ satisfies, $\boldsymbol{\tau}_h \mathbf{n} = \mathbf{0}$ on ∂E , and $\mathbf{div} \boldsymbol{\tau}_h = \mathbf{0}$, which imply $\boldsymbol{\tau}_h = \mathbf{0}$ (cf. (9)). \square

Alternatively, one may consider the following degrees of freedom (useful for the implementation purposes).

- For each edge $e \in \partial E$, given $\boldsymbol{\tau}_h \in \Sigma_h(E)$, the first subset of degrees of freedom is the set of values of $\boldsymbol{\tau}_h \mathbf{n}$ at $k+1$ distinct points in e (for instance, the $k+1$ Gauss-Lobatto nodes). Another possible choice, which has been used in our numerical tests of Section 5 is the following: for each e , we introduce a local linear coordinate $s \in [-1, 1]$; for both components of $\boldsymbol{\tau}_h \in \Sigma_h(E)$, the degrees of freedom are the $k+1$ coefficients of their expansion with respect to the basis $\{1, s, s^2, \dots, s^k\}$.

These $2(k+1)$ values account for the degrees of freedom described in (14).

- In the polygon E , let us choose a basis $\{\boldsymbol{\varphi}_i\}$ ($i = 1, \dots, (k+1)(k+2) - 3$) for RM_k^\perp , see (8). Then, for each $\boldsymbol{\tau}_h \in \Sigma_h(E)$, we may write

$$\mathbf{div} \boldsymbol{\tau}_h = \boldsymbol{\alpha} + \beta(\mathbf{x} - \mathbf{x}_C)^\perp + \sum_{i=1}^{m_k} \gamma_i \boldsymbol{\varphi}_i(\mathbf{x}), \quad (18)$$

where $m_k := (k+1)(k+2) - 3$.

The values $\{\gamma_1, \dots, \gamma_{m_k}\}$ can be taken as the second subset of degrees of freedom. They account for the degrees of freedom described in (15), while $\{\boldsymbol{\alpha}, \beta\}$ are computed according with (13).

The local approximation space for the displacement field is simply defined by, see (6):

$$U_h(E) = \left\{ \mathbf{v}_h \in L^2(E)^2 : \mathbf{v}_h \in \mathcal{P}_k(E)^2 \right\}, \quad (19)$$

and a set of degrees of freedom can be defined in a standard way.

We notice that $\dim(\Sigma_h(E)) = 2(k+1)n_E + m_k$, while $\dim(U_h(E)) = (k+1)(k+2)$. In Figure 1 the local degrees of freedom for stresses and displacements are schematically depicted for $k=1$: arrows represent traction degrees of freedom (cf. (14)), bullets represent the divergence degrees of freedom (cf. (15)), crosses represent the displacement degrees of freedom (cf. (19)).

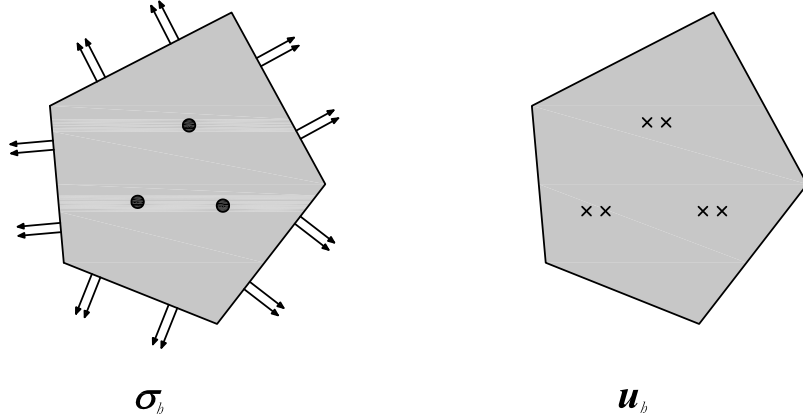


Figure 1: Schematic description of the local degrees of freedom for $k=1$.

3.2 The local bilinear forms

We begin by noticing that, for every $\boldsymbol{\tau}_h \in \Sigma_h(E)$ and $\mathbf{v}_h \in U_h(E)$, the term

$$\int_E \mathbf{div} \boldsymbol{\tau}_h \cdot \mathbf{v}_h \quad (20)$$

is computable. As a consequence, the terms $(\mathbf{div} \boldsymbol{\tau}, \mathbf{u})$ and $(\mathbf{div} \boldsymbol{\sigma}, \mathbf{v})$ in problem (2) are left unaltered. Instead, the term

$$a_E(\boldsymbol{\sigma}_h, \boldsymbol{\tau}_h) = \int_E \mathbb{D} \boldsymbol{\sigma}_h : \boldsymbol{\tau}_h \quad (21)$$

is not computable for a general couple $(\boldsymbol{\sigma}_h, \boldsymbol{\tau}_h) \in \Sigma_h(E) \times \Sigma_h(E)$. In the spirit of the VEM approach (see [8], for instance), we define a suitable approximation $a_E^h(\cdot, \cdot)$. Given $E \in \mathcal{T}_h$, following [4], we first introduce the space:

$$\tilde{\Sigma}(E) := \left\{ \boldsymbol{\tau} \in H(\mathbf{div}; E) : \exists \mathbf{w} \in H^1(E)^2 \text{ such that } \boldsymbol{\tau} = \mathbb{C}\boldsymbol{\varepsilon}(\mathbf{w}) \right\}, \quad (22)$$

and the global space $\tilde{\Sigma}$ as

$$\tilde{\Sigma} := \left\{ \boldsymbol{\tau} \in H(\mathbf{div}; \Omega) : \exists \mathbf{w} \in H^1(\Omega)^2 \text{ such that } \boldsymbol{\tau} = \mathbb{C}\boldsymbol{\varepsilon}(\mathbf{w}) \right\}. \quad (23)$$

We then introduce the projection operator Π_E^k onto the space

$$T_k(E) := \mathbb{C}\boldsymbol{\varepsilon}(\mathcal{P}_{k+1}(E)^2) = \left\{ \mathbb{C}\boldsymbol{\varepsilon}(\mathbf{p}_{k+1}) : \mathbf{p}_{k+1} \in \mathcal{P}_{k+1}(E)^2 \right\} \quad (24)$$

by setting (cf. (22)):

$$\begin{cases} \Pi_E^k : \tilde{\Sigma}(E) \rightarrow T_k(E) \\ \boldsymbol{\tau} \mapsto \Pi_E^k \boldsymbol{\tau} \\ a_E(\Pi_E^k \boldsymbol{\tau}, \boldsymbol{\pi}_k) = a_E(\boldsymbol{\tau}, \boldsymbol{\pi}_k) \quad \forall \boldsymbol{\pi}_k \in T_k(E). \end{cases} \quad (25)$$

We remark that (25) is equivalent to find $\mathbf{p}_{k+1} \in \mathcal{P}_{k+1}(E)^2$ such that

$$\int_E \mathbb{C}\boldsymbol{\varepsilon}(\mathbf{p}_{k+1}) : \boldsymbol{\varepsilon}(\mathbf{q}_{k+1}) = \int_E \boldsymbol{\tau} : \boldsymbol{\varepsilon}(\mathbf{q}_{k+1}) \quad \forall \mathbf{q}_{k+1} \in \mathcal{P}_{k+1}(E)^2. \quad (26)$$

Remark 2. Obviously, \mathbf{p}_{k+1} is defined up to a term in $RM(E)$. In addition, we observe that for \mathbb{C} constant in E , it holds $T_1(E) = \mathcal{P}_1(E)_s^4$; for \mathbb{C} varying in E , $T_k(E)$ is not even a polynomial space.

We have the following proposition.

Proposition 3.2. Fix $k \geq 1$, and let r be such that $0 \leq r \leq k+1$. Under assumptions (A1) and (A2), for the projection operator Π_E^k defined in (25), the following estimates hold:

$$\|\boldsymbol{\tau} - \Pi_E^k \boldsymbol{\tau}\|_{0,E} \lesssim h_E^r |\mathbf{w}|_{r+1,E} \quad \forall \boldsymbol{\tau} \in \tilde{\Sigma}(E) \cap H^r(E)_s^4 \text{ with } \boldsymbol{\tau} = \mathbb{C}\boldsymbol{\varepsilon}(\mathbf{w}). \quad (27)$$

Proof. If $\boldsymbol{\tau} \in \tilde{\Sigma}(E)$, there exists (cf. (22)) $\mathbf{w} \in H^1(E)^2$ such that $\boldsymbol{\tau} = \mathbb{C}\boldsymbol{\varepsilon}(\mathbf{w})$. Inspecting (26), we realize that $\Pi_E^k \boldsymbol{\tau} = \mathbb{C}\boldsymbol{\varepsilon}(\mathbf{p}_{k+1})$, where \mathbf{p}_{k+1} is the Galerkin solution in $\mathcal{P}_{k+1}(E)^2/RM(E)$ of the following Neumann problem.

$$\begin{cases} \text{Find } \mathbf{z} \in H^1(E)^2/RM(E) \text{ s.t.:} \\ \operatorname{div}(\mathbb{C}\boldsymbol{\varepsilon}(\mathbf{z})) = \operatorname{div}(\mathbb{C}\boldsymbol{\varepsilon}(\mathbf{w})) & \text{in } E \\ \mathbb{C}\boldsymbol{\varepsilon}(\mathbf{z})\mathbf{n} = \mathbb{C}\boldsymbol{\varepsilon}(\mathbf{w})\mathbf{n} & \text{on } \partial E. \end{cases} \quad (28)$$

Estimate (27) now follows from standard arguments of the Galerkin technique combined with polynomial approximation results. \square

With the operator Π_E^k at hand, we set

$$\begin{aligned} a_E^h(\boldsymbol{\sigma}_h, \boldsymbol{\tau}_h) &= a_E(\Pi_E^k \boldsymbol{\sigma}_h, \Pi_E^k \boldsymbol{\tau}_h) + s_E \left((Id - \Pi_E^k) \boldsymbol{\sigma}_h, (Id - \Pi_E^k) \boldsymbol{\tau}_h \right) \\ &= \int_E \mathbb{D}(\Pi_E^k \boldsymbol{\sigma}_h) : (\Pi_E^k \boldsymbol{\tau}_h) + s_E \left((Id - \Pi_E^k) \boldsymbol{\sigma}_h, (Id - \Pi_E^k) \boldsymbol{\tau}_h \right), \end{aligned} \quad (29)$$

where $s_E(\cdot, \cdot)$ is a suitable stabilization term. We propose the following choice:

$$s_E(\boldsymbol{\sigma}_h, \boldsymbol{\tau}_h) := \kappa_E h_E \int_{\partial E} \boldsymbol{\sigma}_h \mathbf{n} \cdot \boldsymbol{\tau}_h \mathbf{n}, \quad (30)$$

where κ_E is a positive constant to be chosen (for instance, any norm of $\mathbb{D}|_E$).

3.3 The local loading terms

The loading term, see (2), is simply:

$$(\mathbf{f}, \mathbf{v}_h) = \int_{\Omega} \mathbf{f} \cdot \mathbf{v}_h = \sum_{E \in \mathcal{T}_h} \int_E \mathbf{f} \cdot \mathbf{v}_h. \quad (31)$$

Computing (31) is possible once a suitable quadrature rule is available for polygonal domains (see for instance [21, 22, 20]).

3.4 The discrete scheme

We introduce a global approximation space for the stress field, by glueing the local approximation spaces, see (9):

$$\Sigma_h = \left\{ \boldsymbol{\tau}_h \in H(\mathbf{div}; \Omega) : \boldsymbol{\tau}_h|_E \in \Sigma_h(E) \quad \forall E \in \mathcal{T}_h \right\}. \quad (32)$$

For the global approximation of the displacement field, we take, see (19):

$$U_h = \left\{ \mathbf{v}_h \in L^2(\Omega)^2 : \mathbf{v}_h|_E \in U_h(E) \quad \forall E \in \mathcal{T}_h \right\}. \quad (33)$$

In addition, given a local approximation of $a_E(\cdot, \cdot)$, see (29), we set

$$a_h(\boldsymbol{\sigma}_h, \boldsymbol{\tau}_h) := \sum_{E \in \mathcal{T}_h} a_E^h(\boldsymbol{\sigma}_h, \boldsymbol{\tau}_h). \quad (34)$$

The method we consider is then defined by

$$\begin{cases} \text{Find } (\boldsymbol{\sigma}_h, \mathbf{u}_h) \in \Sigma_h \times U_h \text{ such that} \\ a_h(\boldsymbol{\sigma}_h, \boldsymbol{\tau}_h) + (\mathbf{div} \boldsymbol{\tau}_h, \mathbf{u}_h) = 0 \quad \forall \boldsymbol{\tau}_h \in \Sigma_h \\ (\mathbf{div} \boldsymbol{\sigma}_h, \mathbf{v}_h) = -(\mathbf{f}, \mathbf{v}_h) \quad \forall \mathbf{v}_h \in U_h. \end{cases} \quad (35)$$

4 Stability and convergence analysis

Since some results of the analysis follow the guidelines of the theory developed in [4], we do not provide full details of all the proofs. However, the treatment of the variable material coefficient case is different, and it is reflected in Theorem 4.7. Its proof is thus thoroughly provided.

In the sequel, given a measurable subset $A \subseteq \Omega$ and $r > 2$, we will use the space

$$W^r(A) := \left\{ \boldsymbol{\tau} : \boldsymbol{\tau} \in L^r(A)_s^4, \mathbf{div} \boldsymbol{\tau} \in L^2(A)^2 \right\}, \quad (36)$$

equipped with the obvious norm.

4.1 An interpolation operator for stresses

We now introduce a local interpolation operator $\mathcal{I}_E : W^r(E) \rightarrow \Sigma_h(E)$, the higher-order version of the one introduced in [4]. Given $\boldsymbol{\tau} \in W^r(E)$, $\mathcal{I}_E \boldsymbol{\tau} \in \Sigma_h(E)$ is determined by:

$$\begin{cases} \int_{\partial E} (\mathcal{I}_E \boldsymbol{\tau}) \mathbf{n} \cdot \boldsymbol{\varphi}_k = \int_{\partial E} \boldsymbol{\tau} \mathbf{n} \cdot \boldsymbol{\varphi}_k & \forall \boldsymbol{\varphi}_k \in R_k(\partial E) \\ \int_E \mathbf{div}(\mathcal{I}_E \boldsymbol{\tau}) \cdot \boldsymbol{\psi}_k = \int_E \mathbf{div} \boldsymbol{\tau} \cdot \boldsymbol{\psi}_k & \forall \boldsymbol{\psi}_k \in RM_k^\perp(E). \end{cases} \quad (37)$$

Above, the space $R_k(\partial E)$ is defined by:

$$R_k(\partial E) = \left\{ \boldsymbol{\varphi}_k \in L^2(\partial E)^2 : \boldsymbol{\varphi}_{k|e} \in \mathcal{P}_k(e)^2, \forall e \in \partial E \right\}. \quad (38)$$

If $\boldsymbol{\tau}$ is not sufficiently regular, the integral in the right-hand side of (37) must be seen as a duality between $W^{-\frac{1}{r},r}(\partial E)^2$ and $W^{\frac{1}{r},r'}(\partial E)^2$. If $\boldsymbol{\tau}$ is a regular function, the above conditions are equivalent to require:

$$\begin{cases} \int_e (\mathcal{I}_E \boldsymbol{\tau}) \mathbf{n} \cdot \mathbf{q}_k = \int_e \boldsymbol{\tau} \mathbf{n} \cdot \mathbf{q}_k & \forall \mathbf{q}_k \in \mathcal{P}_k(e)^2, \quad \forall e \in \partial E; \\ \int_E \mathbf{div}(\mathcal{I}_E \boldsymbol{\tau}) \cdot \boldsymbol{\psi}_k = \int_E \mathbf{div} \boldsymbol{\tau} \cdot \boldsymbol{\psi}_k & \forall \boldsymbol{\psi}_k \in RM_k^\perp(E). \end{cases} \quad (39)$$

We remark that, from Lemma 3.1, $\mathcal{I}_E \boldsymbol{\tau} \in \Sigma_h(E)$ is well-defined by conditions (37). The global interpolation operator $\mathcal{I}_h : W^r(\Omega) \rightarrow \Sigma_h$ is then defined by simply glueing the local contributions provided by \mathcal{I}_E . More precisely, we set $(\mathcal{I}_h \boldsymbol{\tau})|_E := \mathcal{I}_E \boldsymbol{\tau}|_E$ for every $E \in \mathcal{T}_h$ and $\boldsymbol{\tau} \in W^r(\Omega)$.

The following *commuting diagram property* is one of the key points in the analysis of the methods.

Proposition 4.1. *Given $k \geq 1$, for the operator $\mathcal{I}_h : W^r(\Omega) \rightarrow \Sigma_h$ introduced above, it holds:*

$$\mathbf{div}(\mathcal{I}_h \boldsymbol{\tau}) = P_h^k(\mathbf{div} \boldsymbol{\tau}) \quad \forall \boldsymbol{\tau} \in W^r(\Omega), \quad (40)$$

where P_h^k denotes the L^2 -projection operator onto the piecewise polynomial functions of degree $\leq k$.

Proof. It is sufficient to prove property (40) locally, in each element $E \in \mathcal{T}_h$. Fix now $\mathbf{q}_k \in \mathcal{P}_k(E)^2$ and $\boldsymbol{\tau} \in W^r(E)$. By the decomposition (8), we write $\mathbf{q}_k = \mathbf{r} + \boldsymbol{\psi}_k$, where $\mathbf{r} \in RM(E)$ and $\boldsymbol{\psi}_k \in RM_k^\perp(E)$. We have:

$$\begin{aligned} \int_E \mathbf{div} \boldsymbol{\tau} \cdot \mathbf{q}_k &= \int_E \mathbf{div} \boldsymbol{\tau} \cdot \mathbf{r} + \int_E \mathbf{div} \boldsymbol{\tau} \cdot \boldsymbol{\psi}_k \\ &= \int_{\partial E} \boldsymbol{\tau} \mathbf{n} \cdot \mathbf{r} + \int_E \mathbf{div} \boldsymbol{\tau} \cdot \boldsymbol{\psi}_k \\ &= \int_{\partial E} (\mathcal{I}_E \boldsymbol{\tau}) \mathbf{n} \cdot \mathbf{r} + \int_E \mathbf{div}(\mathcal{I}_E \boldsymbol{\tau}) \cdot \boldsymbol{\psi}_k && \text{(by (39))} \\ &= \int_E \mathbf{div}(\mathcal{I}_E \boldsymbol{\tau}) \cdot \mathbf{r} + \int_E \mathbf{div}(\mathcal{I}_E \boldsymbol{\tau}) \cdot \boldsymbol{\psi}_k && \text{(integration by parts)} \\ &= \int_E \mathbf{div}(\mathcal{I}_E \boldsymbol{\tau}) \cdot \mathbf{q}_k. && \text{(since } \mathbf{p}_k = \mathbf{r} + \boldsymbol{\psi}_k \text{)} \end{aligned} \quad (41)$$

From (41) and the definition of L^2 -projection operator, we get $\mathbf{div}(\mathcal{I}_E \boldsymbol{\tau}) = P_h^k(\mathbf{div} \boldsymbol{\tau})$ on E . □

4.2 Approximation estimates

For the interpolation operator \mathcal{I}_h , using similar steps to the ones detailed in [4], one can prove the error estimate stated here below.

Proposition 4.2. *Fix $k \geq 1$, and let r be such that $1 \leq r \leq k+1$. Under assumptions (A1) and (A2), for the interpolation operator \mathcal{I}_E defined in (39), the following estimates hold:*

$$\|\boldsymbol{\tau} - \mathcal{I}_E \boldsymbol{\tau}\|_{0,E} \lesssim h_E^r |\boldsymbol{\tau}|_{r,E} \quad \forall \boldsymbol{\tau} \in \tilde{\Sigma}(E) \cap H^r(E)_s^4, \quad (42)$$

$$\|\mathbf{div}(\boldsymbol{\tau} - \mathcal{I}_E \boldsymbol{\tau})\|_{r,E} \lesssim h_E^r |\mathbf{div} \boldsymbol{\tau}|_{r,E} \quad \forall \boldsymbol{\tau} \in \tilde{\Sigma}(E) \cap H^r(E)_s^4 \text{ s.t. } \mathbf{div} \boldsymbol{\tau} \in H^r(E)^2. \quad (43)$$

We remark that, in particular, estimate (43) is a direct consequence of the commuting property (40) and standard approximation results, see [16].

4.3 The *ellipticity-on-the-kernel* and the *inf-sup* conditions

We first notice that (see (32), (9) and (33), (19)):

$$\mathbf{div}(\Sigma_h) \subseteq U_h. \quad (44)$$

As a consequence, introducing the discrete kernel $K_h \subseteq \Sigma_h$:

$$K_h = \{\boldsymbol{\tau}_h \in \Sigma_h : (\mathbf{div} \boldsymbol{\tau}_h, \mathbf{v}_h) = 0 \quad \forall \mathbf{v}_h \in U_h\}, \quad (45)$$

we infer that $K_h \subseteq K$, i.e. $\boldsymbol{\tau}_h \in K_h$ implies $\mathbf{div} \boldsymbol{\tau}_h = \mathbf{0}$ (cf. (5)). Hence, it holds:

$$\|\boldsymbol{\tau}_h\|_{\Sigma} = \|\boldsymbol{\tau}_h\|_0 \quad \forall \boldsymbol{\tau}_h \in K_h. \quad (46)$$

This is essentially the property that leads to the *ellipticity-on-the-kernel* condition:

Proposition 4.3. *For the method described in Section 3, there exists a constant $\alpha > 0$ such that*

$$a_h(\boldsymbol{\tau}_h, \boldsymbol{\tau}_h) \geq \alpha \|\boldsymbol{\tau}_h\|_{\Sigma}^2 \quad \forall \boldsymbol{\tau}_h \in K_h. \quad (47)$$

Remark 3. *Our methods satisfy $K_h \subset K$, where K is defined by (5). As discussed in [10], this property leads to schemes which do not suffer from volumetric locking (see [18], for instance) and can be used also for nearly incompressible materials.*

To continue, the following discrete *inf-sup* condition is a consequence of the *commuting diagram property* (see Proposition 4.1), and of the theory developed in [4].

Proposition 4.4. *Fix an integer $k \geq 1$. Suppose that assumptions (A1) and (A2) are fulfilled. There exists $\beta > 0$ such that*

$$\sup_{\boldsymbol{\tau}_h \in \Sigma_h} \frac{(\mathbf{div} \boldsymbol{\tau}_h, \mathbf{v}_h)}{\|\boldsymbol{\tau}_h\|_{\Sigma}} \geq \beta \|\mathbf{v}_h\|_U \quad \forall \mathbf{v}_h \in U_h. \quad (48)$$

4.4 Error estimates

We need the following estimate, that can be found in [4]. However, we prove it here in details, for the sake of completeness.

Lemma 4.5. *Under assumptions (A1) and (A2), for every $\boldsymbol{\tau}_h \in \Sigma_h(E)$ it holds*

$$h_E^{1/2} \|(I - \Pi_E^k) \boldsymbol{\tau}_h \mathbf{n}\|_{0,\partial E} \lesssim \|(I - \Pi_E^k) \boldsymbol{\tau}_h\|_{0,E} + h_E \|\mathbf{div}((I - \Pi_E) \boldsymbol{\tau}_h)\|_{0,E}. \quad (49)$$

Proof. For $\tau_{\in \Sigma_h(E)}$, set $\xi_h := (I - \Pi_E^k)\tau_h$. By assumptions **(A1)**, take $\mathbf{x}_S \in E$ as the center of the circle with respect to which E is star-shaped. Using also **(A2)**, E can be regularly triangulated by joining \mathbf{x}_S and the vertices of E , thus obtaining a set of triangles T_e , one per each side $e \in \partial E$. For every triangle T_e , let b_e be the standard edge bubble for e (i.e. $b_e = 4\lambda_1\lambda_2$, if the λ_i 's are the barycentric coordinates of the two vertices of e). Finally, define $\varphi \in H^1(E)^2$ by setting $\varphi|_{T_e} = b_e \xi_h \mathbf{n}$. We have:

$$\begin{aligned} \|\xi_h \mathbf{n}\|_{0,\partial E}^2 &\lesssim \int_{\partial E} \xi_h \mathbf{n} \cdot \varphi = \int_E \operatorname{div} \xi_h \cdot \varphi + \int_E \xi_h : \varepsilon(\varphi) \\ &\lesssim h_E \|\operatorname{div} \xi_h\|_{0,E} h_E^{-1} \|\varphi\|_{0,E} + \|\xi_h\|_{0,E} \|\varepsilon(\varphi)\|_{0,E} \\ &\lesssim (h_E \|\operatorname{div} \xi_h\|_{0,E} + \|\xi_h\|_{0,E}) h_E^{-1} \|\varphi\|_{0,E} \\ &\lesssim (h_E \|\operatorname{div} \xi_h\|_{0,E} + \|\xi_h\|_{0,E}) h_E^{-1/2} \|\xi_h \mathbf{n}\|_{0,\partial E}. \end{aligned} \quad (50)$$

Hence, we get

$$h_E^{1/2} \|\xi_h \mathbf{n}\|_{0,\partial E} \lesssim h_E \|\operatorname{div} \xi_h\|_{0,E} + \|\xi_h\|_{0,E}, \quad (51)$$

which is exactly (49). \square

Another useful bound is provided in the lemma that follows.

Lemma 4.6. *Under assumptions **(A1)** and **(A2)**, for every $\tau_h \in \Sigma_h(E)$ the following inverse estimate holds*

$$\|\operatorname{div}(\Pi_E^k \tau_h)\|_{0,E} \lesssim h_E^{-1} \|\tau_h\|_{0,E}. \quad (52)$$

Proof. Let $\Pi_E^k \tau_h = \mathbb{C}\varepsilon(\mathbf{p}_{k+1})$ for a suitable $\mathbf{p}_{k+1} \in \mathcal{P}_{k+1}(E)^2$, see (25)-(26). A direct computation shows that

$$\|\operatorname{div}(\mathbb{C}\varepsilon(\mathbf{p}_{k+1}))\|_{0,E} \lesssim |\mathbb{C}|_{W^{1,\infty}(E)} \|\varepsilon(\mathbf{p}_{k+1})\|_{0,E} + |\mathbb{C}|_{L^\infty(E)} |\varepsilon(\mathbf{p}_{k+1})|_{1,E}. \quad (53)$$

Since $\varepsilon(\mathbf{p}_{k+1})$ is a polynomial of degree at most k for each component, using the techniques in [6], we get $|\varepsilon(\mathbf{p}_{k+1})|_{1,E} \lesssim h_E^{-1} \|\varepsilon(\mathbf{p}_{k+1})\|_{0,E}$. Therefore, from (53), we obtain

$$\begin{aligned} \|\operatorname{div}(\mathbb{C}\varepsilon(\mathbf{p}_{k+1}))\|_{0,E} &\lesssim \left(|\mathbb{C}|_{W^{1,\infty}(E)} + h_E^{-1} |\mathbb{C}|_{L^\infty(E)} \right) \|\varepsilon(\mathbf{p}_{k+1})\|_{0,E} \\ &\lesssim h_E^{-1} \|\varepsilon(\mathbf{p}_{k+1})\|_{0,E} \lesssim h_E^{-1} \|\tau_h\|_{0,E}, \end{aligned} \quad (54)$$

and the proof is complete. \square

We are now ready to present our main convergence result.

Theorem 4.7. *Let k be an integer with $k \geq 1$, and r such that $1 \leq r \leq k+1$. Let $(\sigma, \mathbf{u}) \in \Sigma \times U$ be the solution of Problem (2), and let $(\sigma_h, \mathbf{u}_h) \in \Sigma_h \times U_h$ be the solution of the discrete problem (35). Suppose that assumptions **(A1)** and **(A2)** are fulfilled. Assuming σ and \mathbf{u} sufficiently regular, the following estimate holds true:*

$$\|\sigma - \sigma_h\|_\Sigma + \|\mathbf{u} - \mathbf{u}_h\|_U \lesssim h^r \left(|\sigma|_r + \|\operatorname{div} \sigma\|_r + |\mathbb{C}|_{W^{r,\infty}} \|\sigma\|_0 + \|\mathbf{u}\|_r \right). \quad (55)$$

Proof. We first consider any approximated material tensor \mathbb{C}_h^k , for which it holds

$$h_E |\mathbb{C} - \mathbb{C}_h^k|_{W^{1,\infty}(E)} + \|\mathbb{C} - \mathbb{C}_h^k\|_{L^\infty(E)} \lesssim h_E^r |\mathbb{C}|_{W^{r,\infty}(E)}, \quad 1 \leq r \leq k+1, \quad \forall E \in \mathcal{T}_h. \quad (56)$$

For instance, on each $E \in \mathcal{T}_h$, one may take \mathbb{C}_h^k as the component-wise averaged Taylor expansion of \mathbb{C}_h (see [12], for example).

Take now $\boldsymbol{\sigma}_I = \mathcal{I}_h \boldsymbol{\sigma}$, and notice that $(\boldsymbol{\sigma}_h - \boldsymbol{\sigma}_I) \in K_h \subseteq K$. Hence, using (2) and (35), we infer

$$a(\boldsymbol{\sigma}, \boldsymbol{\sigma}_h - \boldsymbol{\sigma}_I) = a_h(\boldsymbol{\sigma}_I, \boldsymbol{\sigma}_h - \boldsymbol{\sigma}_I) = 0.$$

Therefore, it holds

$$\begin{aligned} \|\boldsymbol{\sigma}_h - \boldsymbol{\sigma}_I\|_\Sigma^2 &= \|\boldsymbol{\sigma}_h - \boldsymbol{\sigma}_I\|_0^2 \lesssim a_h(\boldsymbol{\sigma}_h - \boldsymbol{\sigma}_I, \boldsymbol{\sigma}_h - \boldsymbol{\sigma}_I) \\ &= a(\boldsymbol{\sigma}, \boldsymbol{\sigma}_h - \boldsymbol{\sigma}_I) - a_h(\boldsymbol{\sigma}_I, \boldsymbol{\sigma}_h - \boldsymbol{\sigma}_I) \\ &= a(\boldsymbol{\sigma} - \Pi_h \boldsymbol{\sigma}_I, \boldsymbol{\sigma}_h - \boldsymbol{\sigma}_I) - \sum_{E \in \mathcal{T}_h} s_E((I - \Pi_E^k) \boldsymbol{\sigma}_I, (I - \Pi_E^k)(\boldsymbol{\sigma}_h - \boldsymbol{\sigma}_I)) \\ &= T_1 + T_2, \end{aligned} \quad (57)$$

where we have denoted with Π_h^k the global projector made up by the local contributions Π_E^k , see (25). For the term T_1 , we simply have (cf. (27)):

$$T_1 \lesssim \|\boldsymbol{\sigma} - \Pi_h \boldsymbol{\sigma}_I\|_0 \|\boldsymbol{\sigma}_h - \boldsymbol{\sigma}_I\|_0 \lesssim h^r |\boldsymbol{\sigma}|_r \|\boldsymbol{\sigma}_h - \boldsymbol{\sigma}_I\|_0 \lesssim h^r |\boldsymbol{\sigma}|_r \|\boldsymbol{\sigma}_h - \boldsymbol{\sigma}_I\|_\Sigma. \quad (58)$$

The term T_2 is more involved. Let us treat it locally, on each polygon E . Using Lemma 4.5, we get

$$\begin{aligned} &-s_E((I - \Pi_E^k) \boldsymbol{\sigma}_I, (I - \Pi_E^k)(\boldsymbol{\sigma}_h - \boldsymbol{\sigma}_I)) \\ &\lesssim h_E^{1/2} \|(I - \Pi_E^k) \boldsymbol{\sigma}_I \mathbf{n}\|_{0,\partial E} h_E^{1/2} \|(I - \Pi_E^k)(\boldsymbol{\sigma}_h - \boldsymbol{\sigma}_I) \mathbf{n}\|_{0,\partial E} \\ &\lesssim \left(\|(I - \Pi_E^k) \boldsymbol{\sigma}_I\|_{0,E} + h_E \|\mathbf{div}((I - \Pi_E^k) \boldsymbol{\sigma}_I)\|_{0,E} \right) \times \\ &\quad \left(\|(I - \Pi_E^k)(\boldsymbol{\sigma}_h - \boldsymbol{\sigma}_I)\|_{0,E} + h_E \|\mathbf{div}((I - \Pi_E^k)(\boldsymbol{\sigma}_h - \boldsymbol{\sigma}_I))\|_{0,E} \right) \end{aligned} \quad (59)$$

Recalling that $\mathbf{div}(\boldsymbol{\sigma}_h - \boldsymbol{\sigma}_I) = \mathbf{0}$ and using Lemma 4.6, we infer

$$h_E \|\mathbf{div}((I - \Pi_E^k)(\boldsymbol{\sigma}_h - \boldsymbol{\sigma}_I))\|_{0,E} \lesssim \|\boldsymbol{\sigma}_h - \boldsymbol{\sigma}_I\|_{0,E}. \quad (60)$$

The L^2 continuity of Π_E^k , combined with (59) and (60), gives

$$\begin{aligned} &-s_E((I - \Pi_E^k) \boldsymbol{\sigma}_I, (I - \Pi_E^k)(\boldsymbol{\sigma}_h - \boldsymbol{\sigma}_I)) \\ &\lesssim \left(\|(I - \Pi_E^k) \boldsymbol{\sigma}_I\|_{0,E} + h_E \|\mathbf{div}((I - \Pi_E^k) \boldsymbol{\sigma}_I)\|_{0,E} \right) \|\boldsymbol{\sigma}_h - \boldsymbol{\sigma}_I\|_{0,E} \\ &\lesssim \left(\|(I - \Pi_E^k) \boldsymbol{\sigma}_I\|_{0,E} + h_E \|\mathbf{div}((I - \Pi_E^k) \boldsymbol{\sigma}_I)\|_{0,E} \right) \|\boldsymbol{\sigma}_h - \boldsymbol{\sigma}_I\|_{\Sigma(E)}. \end{aligned} \quad (61)$$

We now estimate $\|(I - \Pi_E^k) \boldsymbol{\sigma}_I\|_{0,E} + h_E \|\mathbf{div}((I - \Pi_E^k) \boldsymbol{\sigma}_I)\|_{0,E}$. We first have

$$\begin{aligned} \|(I - \Pi_E^k)\sigma_I\|_{0,E} &\leq \|(I - \Pi_E^k)(\sigma_I - \sigma)\|_{0,E} + \|(I - \Pi_E^k)\sigma\|_{0,E} \\ &\lesssim \|\sigma_I - \sigma\|_{0,E} + h_E^r |\sigma|_{r,E} \lesssim h_E^r |\sigma|_{r,E}, \end{aligned} \quad (62)$$

where we have also used estimates (27) and (42). To treat the term

$$h_E \|\mathbf{div}((I - \Pi_E^k)\sigma_I)\|_{0,E} \quad (63)$$

we argue as follows.

Let $\mathbf{q} \in \mathcal{P}_{k+1}(E)^2$ be such that $\mathbb{C}\varepsilon(\mathbf{q}) = \Pi_E^k \sigma_I$. We write

$$\begin{aligned} h_E \|\mathbf{div}((I - \Pi_E^k)\sigma_I)\|_{0,E} &= h_E \|\mathbf{div} \sigma_I - \mathbf{div}(\mathbb{C}\varepsilon(\mathbf{q}))\|_{0,E} \\ &\leq h_E \|\mathbf{div}(\sigma_I - \mathbb{C}_h^k \varepsilon(\mathbf{q}))\|_{0,E} + h_E \|\mathbf{div}((\mathbb{C}_h^k - \mathbb{C})\varepsilon(\mathbf{q}))\|_{0,E} = D_1 + D_2. \end{aligned} \quad (64)$$

Since $\mathbf{div}(\sigma_I - \mathbb{C}_h^k \varepsilon(\mathbf{q}))$ is polynomial in E , the techniques of [6] can be used to get the inverse estimate

$$D_1 \lesssim \|\sigma_I - \mathbb{C}_h^k \varepsilon(\mathbf{q})\|_{0,E}. \quad (65)$$

Since, using (27), (42) and (56), we get

$$\begin{aligned} \|\sigma_I - \mathbb{C}_h^k \varepsilon(\mathbf{q})\|_{0,E} &\leq \|\sigma_I - \Pi_E^k \sigma_I\|_{0,E} + \|(\mathbb{C} - \mathbb{C}_h^k)\varepsilon(\mathbf{q})\|_{0,E} \\ &\leq \|(I - \Pi_E^k)(\sigma_I - \sigma)\|_{0,E} + \|(I - \Pi_E^k)\sigma\|_{0,E} + h_E^r |\mathbb{C}|_{W^{r,\infty}(E)} \|\varepsilon(\mathbf{q})\|_{0,E} \\ &\lesssim \|\sigma_I - \sigma\|_{0,E} + h_E^r |\sigma|_{r,E} + h_E^r |\mathbb{C}|_{W^{r,\infty}(E)} \|\sigma_I\|_{0,E} \lesssim h_E^r (1 + |\mathbb{C}|_{W^{r,\infty}(E)}) |\sigma|_{r,E}, \end{aligned} \quad (66)$$

we infer that it holds

$$D_1 \lesssim h_E^r (1 + |\mathbb{C}|_{W^{r,\infty}(E)}) |\sigma|_{r,E} \lesssim h_E^r |\sigma|_{r,E}. \quad (67)$$

To treat D_2 , a direct computation shows that

$$D_2 \lesssim h_E \left(|\mathbb{C} - \mathbb{C}_h^k|_{W^{1,\infty}(E)} \|\sigma_I\|_{0,E} + \|\mathbb{C} - \mathbb{C}_h^k\|_{L^\infty(E)} |\varepsilon(\mathbf{q})|_{1,E} \right). \quad (68)$$

Using an inverse estimate for polynomials on polygons, see [6], and estimate (56), we get

$$D_2 \lesssim h_E |\mathbb{C} - \mathbb{C}_h^k|_{W^{1,\infty}(E)} \|\sigma_I\|_{0,E} + \|\mathbb{C} - \mathbb{C}_h^k\|_{L^\infty(E)} |\varepsilon(\mathbf{q})|_{0,E} \lesssim h_E^r |\mathbb{C}|_{W^{r,\infty}(E)} \|\sigma_I\|_{0,E}. \quad (69)$$

From estimate (42) and the triangle inequality we obtain

$$D_2 \lesssim h_E^r |\mathbb{C}|_{W^{r,\infty}(E)} (\|\sigma\|_{0,E} + h_E^r |\sigma|_{r,E}). \quad (70)$$

Combining (64), (67) and (70), we have

$$h_E \|\mathbf{div}((I - \Pi_E^k)\sigma_I)\|_{0,E} \lesssim h_E^r \left(|\sigma|_{r,E} + |\mathbb{C}|_{W^{r,\infty}(E)} \|\sigma\|_{0,E} \right) \quad (71)$$

From estimate (61), (62) and (71) we deduce

$$-s_E((I - \Pi_E^k)\sigma_I, (I - \Pi_E^k)(\sigma_h - \sigma_I)) \lesssim h_E^r \left(|\sigma|_{r,E} + |\mathbb{C}|_{W^{r,\infty}(E)} \|\sigma\|_{0,E} \right) \|\sigma_h - \sigma_I\|_{\Sigma(E)}. \quad (72)$$

Summing up all the local contributions (cf. also (57)), one gets

$$T_2 \lesssim h^r \left(|\sigma|_r + |\mathbb{C}|_{W^{r,\infty}} \|\sigma\|_0 \right) \|\sigma_h - \sigma_I\|_{\Sigma}. \quad (73)$$

Using (58), (73), from (57) we infer

$$\|\sigma_h - \sigma_I\|_{\Sigma} \lesssim h^r \left(|\sigma|_r + |\mathbb{C}|_{W^{r,\infty}} \|\sigma\|_0 \right). \quad (74)$$

The triangle inequality and estimates (42)-(43) now give

$$\|\sigma - \sigma_h\|_{\Sigma} \lesssim h^r \left(|\sigma|_r + |\mathbf{div} \sigma|_r + |\mathbb{C}|_{W^{r,\infty}} \|\sigma\|_0 \right). \quad (75)$$

We now estimate $\|\mathbf{u} - \mathbf{u}_h\|_U$. We set \mathbf{u}_I as the L^2 -projection of \mathbf{u} onto the subspace U_h . The *inf-sup* condition (48) implies that there exists $\tau_h \in \Sigma_h$ such that

$$\|\mathbf{u}_h - \mathbf{u}_I\|_U \lesssim (\mathbf{div} \tau_h, \mathbf{u}_h - \mathbf{u}_I) = (\mathbf{div} \tau_h, \mathbf{u}_h - \mathbf{u}), \quad \tau_h \lesssim 1. \quad (76)$$

Using (35) and (2), we get

$$\|\mathbf{u}_h - \mathbf{u}_I\|_U \lesssim a(\sigma, \tau_h) - a_h(\sigma_h, \tau_h). \quad (77)$$

To estimate the right-hand side of (77), we proceed locally on each polygon E . We thus have to consider

$$a_E(\sigma, \tau_h) - a_E(\Pi_E^k \sigma_h, \Pi_E^k \tau_h) - s_E((I - \Pi_E^k) \sigma_h, (I - \Pi_E^k) \tau_h). \quad (78)$$

It is immediate to see that

$$a_E(\sigma, \tau_h) - a_E(\Pi_E^k \sigma_h, \Pi_E^k \tau_h) \lesssim \|\sigma - \sigma_h\|_{\Sigma(E)} \|\tau_h\|_{\Sigma(E)}. \quad (79)$$

Similarly to (59), we have

$$\begin{aligned} & -s_E((I - \Pi_E^k) \sigma_h, (I - \Pi_E^k) \tau_h) \\ & \lesssim \left(\|(I - \Pi_E^k) \sigma_h\|_{0,E} + h_E \|\mathbf{div}((I - \Pi_E^k) \sigma_h)\|_{0,E} \right) \times \\ & \quad \left(\|(I - \Pi_E^k) \tau_h\|_{0,E} + h_E \|\mathbf{div}((I - \Pi_E^k) \tau_h)\|_{0,E} \right). \end{aligned} \quad (80)$$

Using the same arguments as in (68)-(69), we get

$$h_E \|\mathbf{div}((I - \Pi_E^k) \tau_h)\|_{0,E} \lesssim h_E \|\mathbf{div} \tau_h\|_{0,E} + \|\tau_h\|_{0,E} \lesssim \|\tau_h\|_{\Sigma(E)}. \quad (81)$$

Due to the L^2 -continuity of Π_E^k , we deduce

$$\|(I - \Pi_E^k) \tau_h\|_{0,E} + h_E \|\mathbf{div}((I - \Pi_E^k) \tau_h)\|_{0,E} \lesssim \|\tau_h\|_{\Sigma(E)}. \quad (82)$$

The term $\|(I - \Pi_E^k) \sigma_h\|_{0,E} + h_E \|\mathbf{div}((I - \Pi_E^k) \sigma_h)\|_{0,E}$ can be treated by adding and subtracting σ_I , and then by using (60), (62) (71). Hence, we have

$$\begin{aligned} & \|(I - \Pi_E^k) \sigma_h\|_{0,E} + h_E \|\mathbf{div}((I - \Pi_E^k) \sigma_h)\|_{0,E} \\ & \leq \|(I - \Pi_E^k)(\sigma_h - \sigma_I)\|_{0,E} + h_E \|\mathbf{div}((I - \Pi_E^k)(\sigma_h - \sigma_I))\|_{0,E} \\ & \quad + \|(I - \Pi_E^k) \sigma_I\|_{0,E} + h_E \|\mathbf{div}((I - \Pi_E^k) \sigma_I)\|_{0,E} \\ & \lesssim \|\sigma_h - \sigma_I\|_{\Sigma(E)} + h_E^r \left(|\sigma|_{r,E} + |\mathbb{C}|_{W^{r,\infty}(E)} \|\sigma\|_{0,E} \right). \end{aligned} \quad (83)$$

From (80), (82) and (82), summing over all the contributions and using (74), we deduce

$$- \sum_{E \in \mathcal{T}_h} s_E((I - \Pi_E^k)\sigma_h, (I - \Pi_E^k)\tau_h) \lesssim h^r \left(|\sigma|_r + |\mathbb{C}|_{W^{r,\infty}} \|\sigma\|_0 \right) \|\tau_h\|_\Sigma. \quad (84)$$

From (77), (79) (84), recalling that $\|\tau_h\|_\Sigma \lesssim 1$, and using (75), we get

$$\|\mathbf{u}_h - \mathbf{u}_I\|_U \lesssim h^r \left(|\sigma|_r + |\mathbf{div} \sigma|_r + |\mathbb{C}|_{W^{r,\infty}} \|\sigma\|_0 \right). \quad (85)$$

Now, the triangle inequality, standard approximation estimates, together with bounds (75) and (85), give (55). \square

Supposing full regularity of the analytical solution, Theorem 4.7 obviously implies the convergence of order $k + 1$:

Corollary 4.8. *Let k be an integer with $k \geq 1$. Let $(\sigma, \mathbf{u}) \in \Sigma \times U$ be sufficiently regular. Let $(\sigma_h, \mathbf{u}_h) \in \Sigma_h \times U_h$ be the solution of the discrete problem (35). Suppose that assumptions (A1) and (A2) are fulfilled. Then*

$$\|\sigma - \sigma_h\|_\Sigma + \|\mathbf{u} - \mathbf{u}_h\|_U \lesssim h^{k+1}. \quad (86)$$

Remark 4. *Another consequence of $K_h \subset K$ (cf. Remark 3) is that the error estimate on the stress field does not depend on the displacement approximation space, see (75). For details about such a point in an abstract framework, we refer to [10], for instance.*

5 Numerical results

In this section the proposed methodology is tested by assessing its accuracy on a selection of problems. Numerical results confirm the soundness of the proposed approach and its optimal performance.

5.1 Accuracy assessment

Three boundary value problems are considered on the unit square domain $\Omega = [0, 1]^2$ assumed to be in plane strain regime. Firstly, the material is assumed to be homogeneous and isotropic with material parameters assigned in terms of the Lamé constants, here set as $\lambda = 1$ and $\mu = 1$ [15, 2]. A required solution is chosen in terms of displacement fields and the corresponding body load \mathbf{f} is consequently obtained as synthetically indicated in the following:

- Test a

$$\begin{cases} u_1 = x^3 - 3xy^2 \\ u_2 = y^3 - 3x^2y \\ \mathbf{f} = \mathbf{0} \end{cases} \quad (87)$$

- Test b

$$\begin{cases} u_1 = u_2 = \sin(\pi x) \sin(\pi y) \\ f_1 = f_2 = -\pi^2 [-(3\mu + \lambda) \sin(\pi x) \sin(\pi y) + (\mu + \lambda) \cos(\pi x) \cos(\pi y)]. \end{cases} \quad (88)$$

It can be noticed that Test *a* is a problem with polynomial solution, non-homogeneous Dirichlet boundary conditions and zero loading; whereas Test *b* has a trigonometric solution, homogeneous Dirichlet boundary conditions and trigonometric distributed loads.

In addition, a case with non-homogeneous material properties is analysed and denoted as Test *c* in the following. Such a case shares the same analytical solution adopted for Test *a* in terms of displacement fields, but material properties are imposed as:

$$\lambda = \mu = 1 - d_c^2(\mathbf{x}), \quad (89)$$

being \mathbf{x} the position vector and d_c^2 the square distance from the centre of the domain (i.e. the point $\mathbf{x} = [0.5, 0.5]$).

Eight meshes characterized by different element topologies and distortion (see Fig. 2) are adopted in order to assess the robustness of the proposed approach. The first four meshes are *structured* and composed of triangles, quadrilaterals, hexagons and a mix of convex and concave quadrilaterals, respectively. Such meshes are denoted in the following by the letter "S". The second four meshes, representing *unstructured* analogues of the first ones, are composed of triangles, quadrilaterals, random polygons and a mix of convex and concave hexagons. Such meshes are denoted in the following by the letter "U". The mesh size parameter used in the following numerical tests is chosen as the average edge length, denoted with \bar{h}_e . It is noticed that, under mesh assumptions (A1) and (A2) and for a quasi-uniform family of mesh, \bar{h}_e is equivalent to both h_E and h . It should be remarked that, with the exception of Test *c*, the same meshes and tests have been used by the authors for the assessment of the low order counterpart of the present general formulation, see [4].

The following error norms are used in order to assess the accuracy and the convergence rate:

- Discrete error norms for the stress field:

$$E_{\boldsymbol{\sigma}} := \left(\sum_{e \in \mathcal{E}_h} |e| \int_e \kappa |(\boldsymbol{\sigma} - \boldsymbol{\sigma}_h) \mathbf{n}|^2 \right)^{1/2}, \quad (90)$$

where $\kappa = \frac{1}{2} \text{tr}(\mathbb{D})$. We remark that the quantity above scales like the internal elastic energy, with respect to the size of the domain and of the elastic coefficients.

We make also use of the L^2 error on the divergence:

$$E_{\boldsymbol{\sigma}, \text{div}} := \left(\sum_{E \in \mathcal{T}_h} \int_E |\text{div}(\boldsymbol{\sigma} - \boldsymbol{\sigma}_h)|^2 \right)^{1/2}. \quad (91)$$

- L^2 error norm for the displacement field:

$$E_{\mathbf{u}} := \left(\sum_{E \in \mathcal{T}_h} \int_E |\mathbf{u} - \mathbf{u}_h|^2 \right)^{1/2} = \|\mathbf{u} - \mathbf{u}_h\|_0. \quad (92)$$

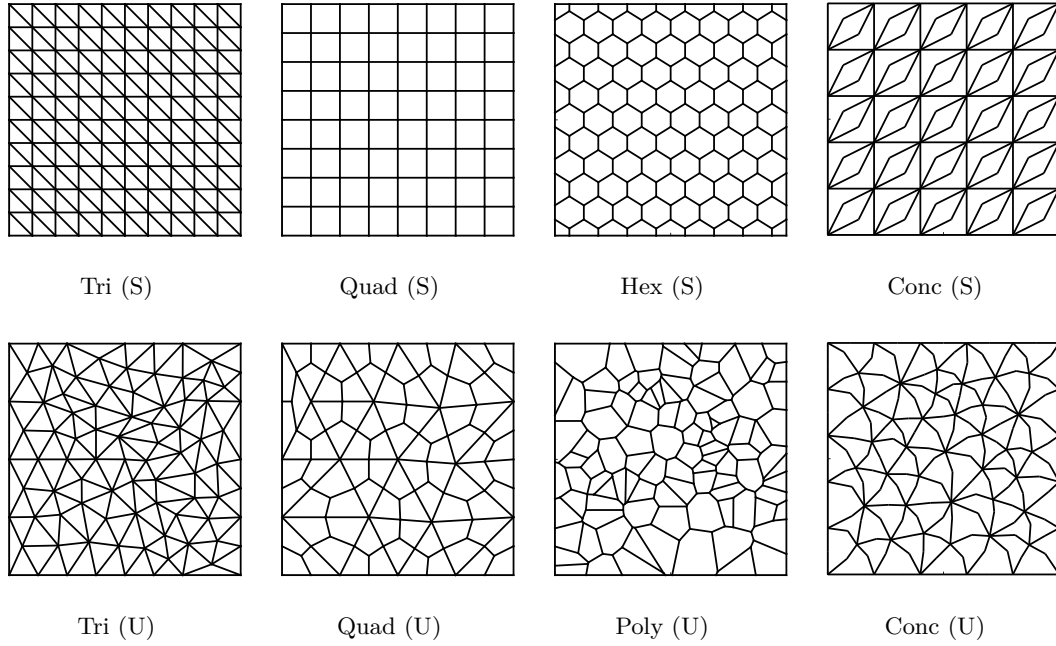


Figure 2: Overview of the adopted meshes in the numerical tests for the convergence assessment.

5.2 Results for $k = 1$

Figure 3 reports the \bar{h}_e -convergence of the proposed method for Test *a* when k is equal to 1. The asymptotic convergence rate is approximately equal to 2 for all the considered error norms and meshes, as expected. The $E_{\sigma, \text{div}}$ plots are not reported for this case because such a quantity is captured up to machine precision for all the considered computational grids.

Figures 4 and 5 report \bar{h}_e -convergence for Test *b* and Test *c*. Asymptotic convergence rate is approximately equal to 2 for all investigated mesh types and error measures. These results highlight the expected optimal performance of the proposed VEM approach and its robustness with respect to the adopted computational grid.

5.3 Results for $k = 2$

Figure 6 reports the \bar{h}_e -convergence of the proposed method for Test *a* when k is equal to 2. The asymptotic convergence rate is approximately equal to 3 for all the considered error norms and meshes, as expected. In this case the E_{σ} and $E_{\sigma, \text{div}}$ plots are not reported because such quantities are captured up to machine precision for all the considered computational grids.

Figure 7 and 8 report \bar{h}_e -convergence for Test *b* and Test *c*. Also in this case results confirm the soundness of the proposed approach.

6 Conclusions

We have presented a family of Virtual Element schemes for the linear elasticity 2D problem, described by the mixed Hellinger-Reissner variational principle. The approximated stresses are *a priori* symmetric and the corresponding tractions are continuous

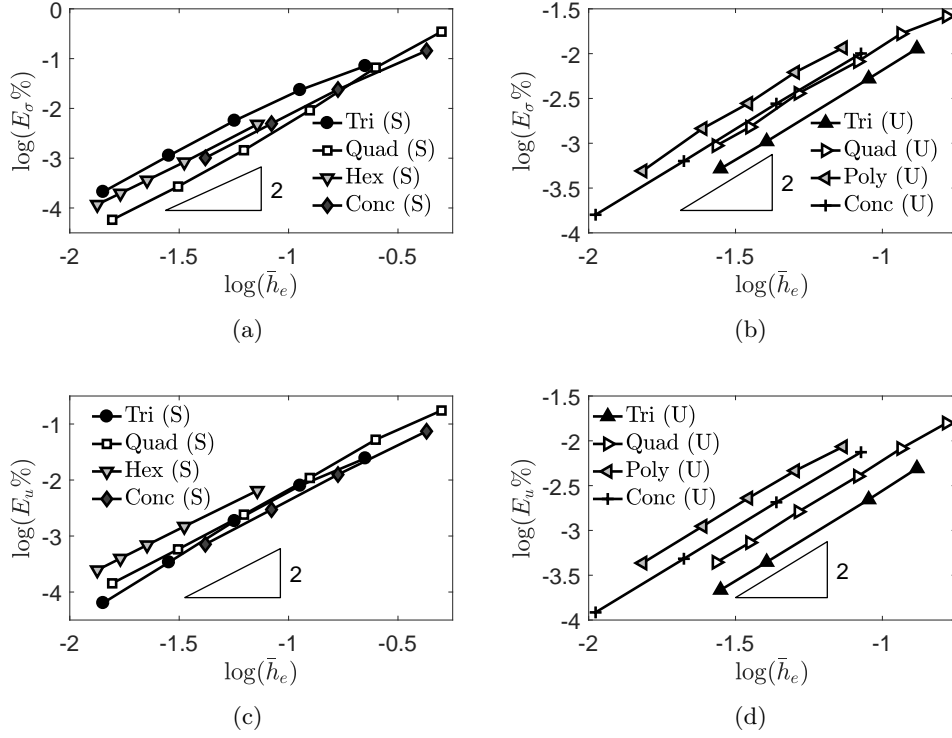


Figure 3: \bar{h}_e -convergence results for Test *a* on structured and unstructured meshes for $k = 1$: (a) and (b) E_σ error norm plots, (c) and (d) E_u error norm plots.

across the polygon inter-elements. We have proved that our methods are stable and optimal convergent, and we have reported some numerical tests that confirm the theoretical predictions. A possible interesting evolution of this paper could be the extension of the present approach to the *three-dimensional* case.

References

- [1] O. Andersen, H. M. Nilsen, and X. Raynaud, *On the use of the virtual element method for geomechanics on reservoir grids*, online: <https://arxiv.org/abs/1606.09508>.
- [2] E. Artioli, L. Beirão da Veiga, C. Lovadina, and E. Sacco, *Arbitrary order 2D virtual elements for polygonal meshes: Part I, elastic problem*, Computational Mechanics **60** (2017), 355–377.
- [3] E. Artioli, L. Beirão da Veiga, C. Lovadina, and E. Sacco, *Arbitrary order 2D virtual elements for polygonal meshes: Part II, inelastic problem*, Computational Mechanics **60** (2017), 643–657.
- [4] E. Artioli, S. de Miranda, C. Lovadina, and L. Patruno, *A stress/displacement virtual element method for plane elasticity problems*, Comput. Methods Appl. Mech. Engrg. **325** (2017), 155–174.
- [5] L. Beirão da Veiga, F. Brezzi, and L. D. Marini, *Virtual Elements for linear elasticity problems*, Siam. J. Numer. Anal. **51** (2013), 794–812.

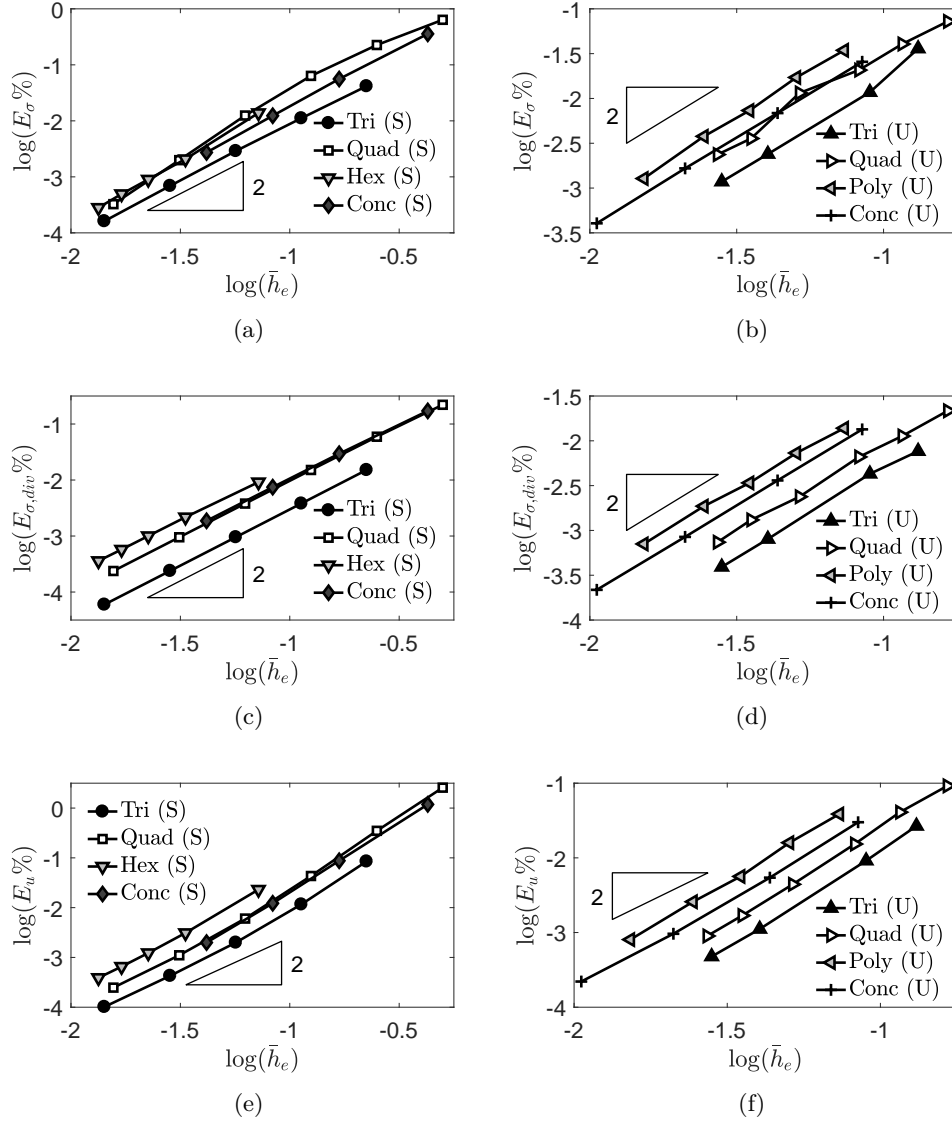


Figure 4: \bar{h}_e -convergence results for Test *b* on structured and unstructured meshes for $k = 1$: (a) and (b) E_{σ} error norm plots, (c) and (d) $E_{\sigma, \text{div}}$ error norm plots, (e) and (f) $E_{\mathbf{u}}$ error norm plots.

- [6] L. Beirão da Veiga, C. Lovadina, and A. Russo, *Stability analysis for the Virtual Element Methods*, Math. Models Methods Appl. Sci. **27** (2017), no. 13, 2557–2594.
- [7] L. Beirão da Veiga and G. Manzini, *A Virtual Element Method with arbitrary regularity*, IMA J. Numer. Anal. **34** (2014), no. 2, 759–781.
- [8] L. Beirão da Veiga, F. Brezzi, A. Cangiani, G. Manzini, L. D. Marini, and A. Russo, *Basic principles of virtual element methods*, Math. Models Methods Appl. Sci. **23** (2013), no. 1, 199–214.
- [9] L. Beirão Da Veiga, C. Lovadina, and G. Vacca, *Divergence free virtual elements for the Stokes problem on polygonal meshes*, ESAIM: M2AN **51** (2017), 509–535.

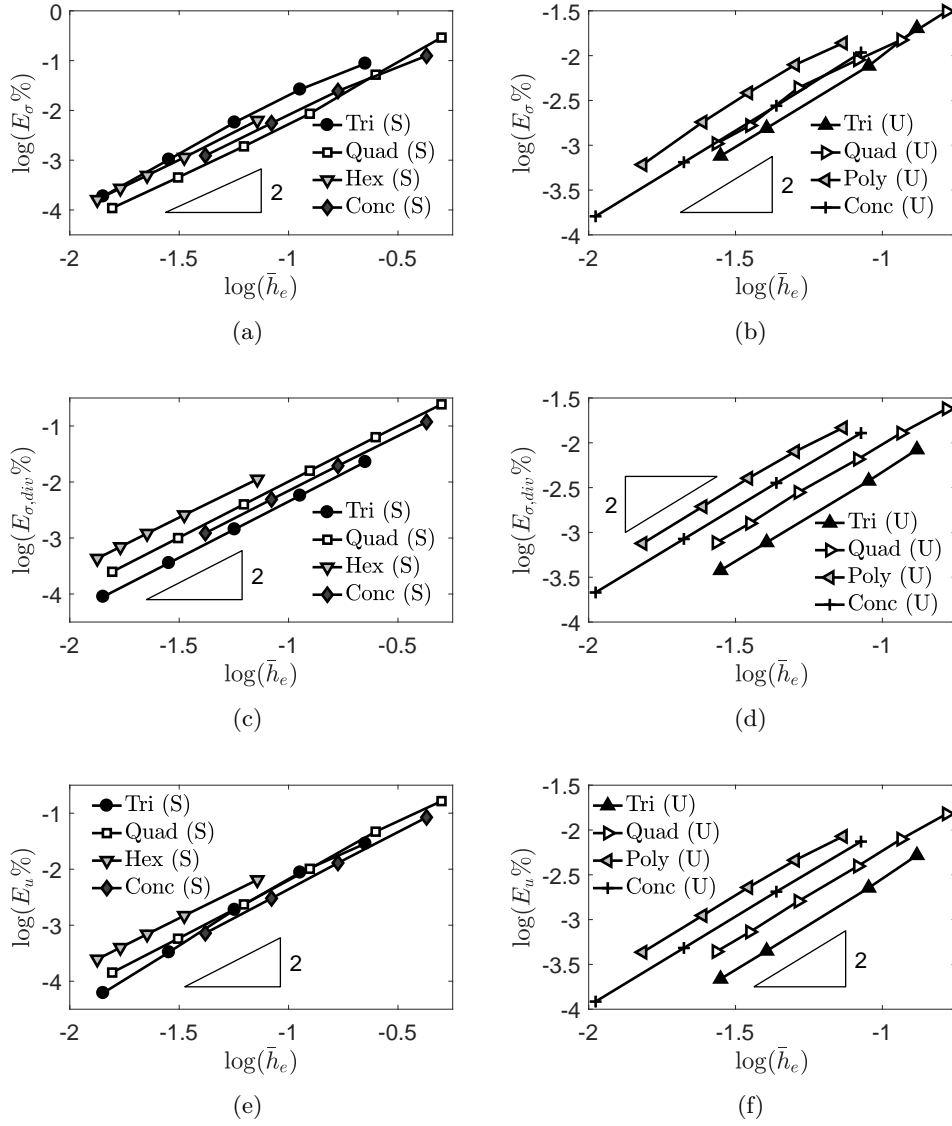


Figure 5: \bar{h}_e -convergence results for Test *c* on structured and unstructured meshes for $k = 1$: (a) and (b) E_{σ} error norm plots, (c) and (d) $E_{\sigma, \text{div}}$ error norm plots, (e) and (f) $E_{\mathbf{u}}$ error norm plots.

- [10] D. Boffi, F. Brezzi, and M. Fortin, *Mixed finite element methods and applications*, Springer Series in Computational Mathematics, vol. 44, Springer, Heidelberg, 2013.
- [11] D. Braess, *Finite elements. Theory, fast solvers, and applications in elasticity theory.*, third ed., Cambridge University Press, 2007.
- [12] S.C. Brenner and L.R. Scott, *The Mathematical Theory of Finite Element Methods*, 3 ed., Texts in Applied Mathematics, Springer, 2008.
- [13] F. Brezzi and L.D. Marini, *Virtual Element Method for plate bending problems*, Comput. Methods Appl. Mech. Engrg. **253** (2012), 455–462.

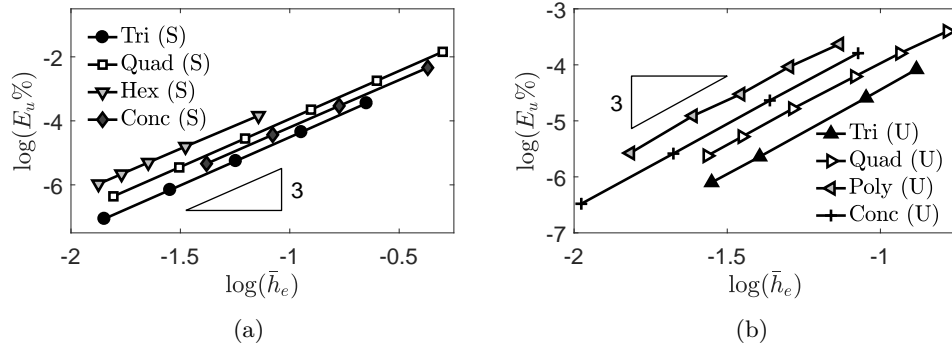


Figure 6: \bar{h}_e –convergence results for Test *a* on structured and unstructured meshes for $k = 2$: (a) and (b) E_u error norm plots.

- [14] H. Chi, L. Beirão da Veiga, and G. H. Paulino, *Some basic formulations of the virtual element method (vem) for finite deformations*, Comput. Meth. Appl. Mech. Engrg., in press.
- [15] L. Beirão da Veiga, C. Lovadina, and D. Mora, *A virtual element method for elastic and inelastic problems on polytope meshes*, Computer Methods in Applied Mechanics and Engineering **295** (2015), 327 – 346.
- [16] T. Dupont and R. Scott, *Polynomial approximation of functions in Sobolev spaces*, Math. Comp. **34** (1980), no. 150, 441–463.
- [17] A. L. Gain, C. Talischi, and G. H. Paulino, *On the virtual element method for three-dimensional linear elasticity problems on arbitrary polyhedral meshes*, Comput. Methods Appl. Mech. Engrg. **282** (2014), 132–160. MR 3269894
- [18] T. J. R. Hughes, *The finite element method. linear static and dynamic finite element analysis.*, second ed., Dover, 2000.
- [19] J.-L. Lions and E. Magenes, *Problèmes aux limites non homogènes et applications. Vol. 1*, Travaux et Recherches Mathématiques, No. 17, Dunod, Paris, 1968.
- [20] S. E. Mousavi and N. Sukumar, *Numerical integration of polynomials and discontinuous functions on irregular convex polygons and polyhedrons*, Computational Mechanics **47** (2011), no. 5, 535–554.
- [21] S. E. Mousavi, H. Xiao, and N. Sukumar, *Generalized Gaussian quadrature rules on arbitrary polygons*, International Journal for Numerical Methods in Engineering **82** (2010), no. 1, 99–113.
- [22] A. Sommariva and M. Vianello, *Product Gauss cubature over polygons based on green’s integration formula*, BIT Numerical Mathematics **47** (2007), no. 2, 441–453.
- [23] P. Wriggers, W.T. Rust, and B.D. Reddy, *A virtual element method for contact*, Comput Mech **58** (2016), 1039–1050.

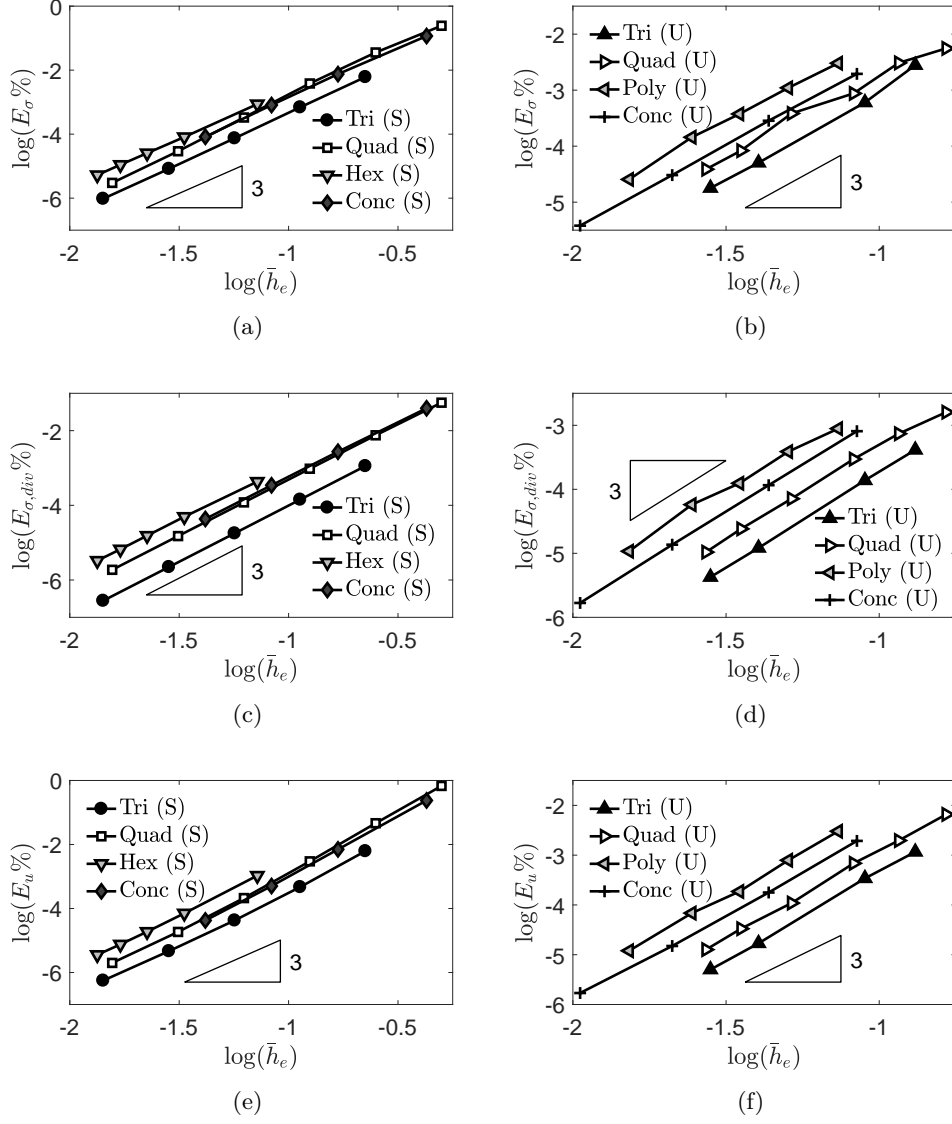


Figure 7: \bar{h}_e -convergence results for Test b on structured and unstructured meshes for $k = 2$: (a) and (b) E_σ error norm plots, (c) and (d) $E_{\sigma,div}$ error norm plots, (e) and (f) E_u error norm plots.

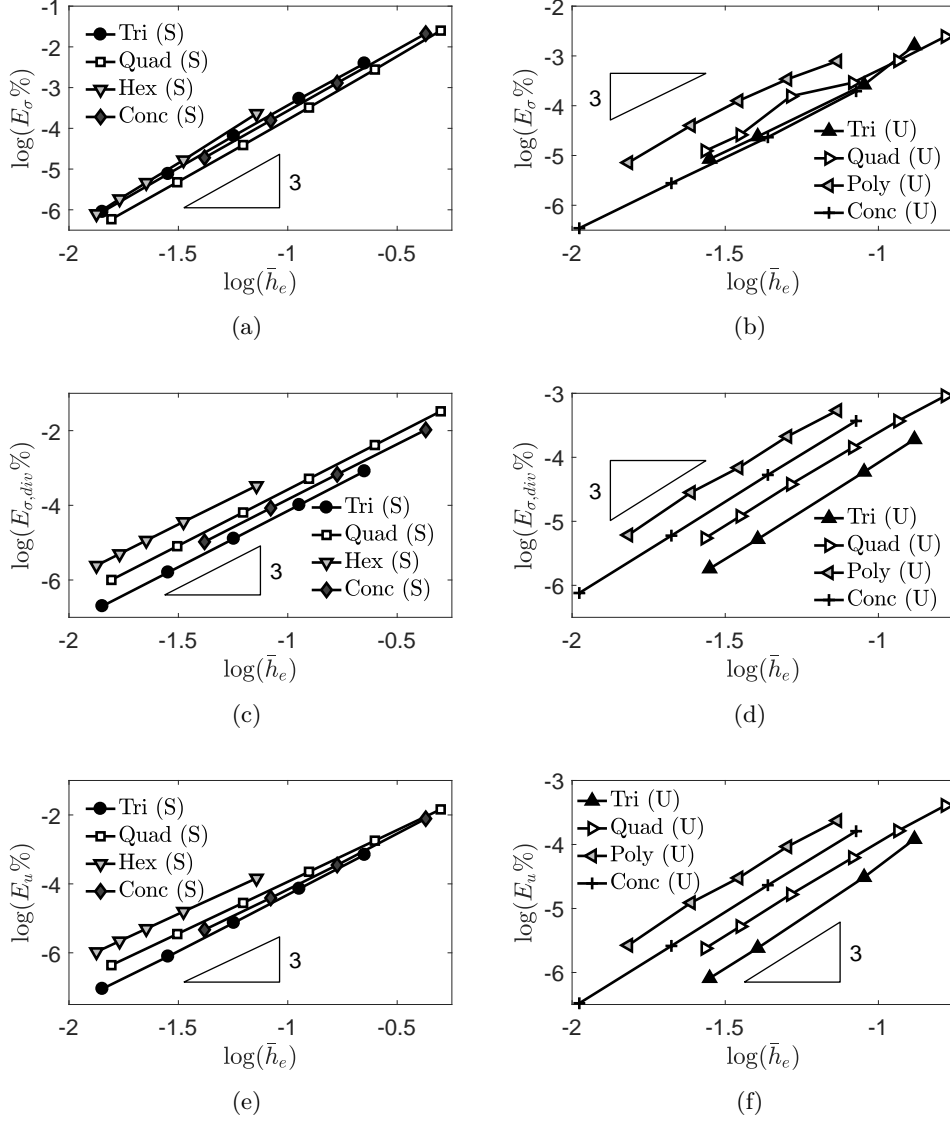


Figure 8: \bar{h}_e -convergence results for Test *c* on structured and unstructured meshes for $k = 2$: (a) and (b) E_σ error norm plots, (c) and (d) $E_{\sigma,div}$ error norm plots, (e) and (f) E_u error norm plots.